ICWE14 June 21-26, 2015 | Porto Alegre - Brazil
14th INTERNATIONAL CONFERENCE ON WIND ENGINEERING

Description of Intensity of Turbulence *IT* in dependence with stability regime at *swept area* of *wind* turbines blades heights.

Alejandro Gutierrez Arce[1]
[1]Instituto de Mecánica de los Fluidos e Ingeniería Ambiental, Facultad de Ingeniería,
Universidad de la República, Montevideo Uruguay.
email: aguti@fing.edu.uy

ABSTRACT: The present work analyzes wind measurements made for wind energy, the analysis focuses on the mean velocity of at heights between 40 and 100 m, at *swept area of a wind turbines blades* . Stability are discriminated by the vertical gradient of temperature. The diurnal cycle of stability is compared among locations with different mesoscale conditions, continental, ocean coast, and estuary coast locations. After sunrise, regimes with a superadiabatic gradient of temperature $\frac{\delta T}{\delta z}$ are observed frequently, stable regimes at night show higher spread of $\frac{\delta T}{\delta z}$. Strong stability is observed at tower locations far from the ocean coast at night. Intensity of Turbulence *IT* is described in dependence with stability regimes, for different season. The peak of intensity of turbulence *IT* is related with unstable regimes. *IT* have a more significance dispersion in ocean coast tower. When mean velocity is extreme the stability regime is slightly unstable,and the *IT* tend to reach a clear asymptotic value of *IT* =0,1 for two tower analyzed Rosendo Mendoza and Colonia Rubio. Also in this work it is proposed a model for computing *IT* based in numerical simulation, with the ratio between *ust (*friction velocity) and mean velocity $\bar{V}$ computed by WRF,a k_{IT} dimensionless coefficient is defined for better adjust related with local mesoscale regimes. The propose model show that diurnal cycle of *IT* can be simulated. Power of 2014 production of Kentilux wind farm (17,2 MW) was analyzed in terms of seasons and diurnal cycle. Mean power production production of wind farm tend to decrease during unstable regime (day time), for all seasons, when in diurnal cycle, mean velocity at *swept area of a wind turbines blades* is minimum and *IT* is maximum.

KEY WORDS: intensity of turbulence, stability.

1 INTRODUCTION

This work analyzes observational data recorded by the National Electric Company of Uruguay (UTE) in their assessment of wind energy resources. Uruguay is dominated by rolling plains and low ranges. Observation towers of wind energy are located in three geographical regions: 1) the region close to the Río de la Plata (an estuary comprising seawater and freshwater from the Paraná River, one of the world's longest rivers, and its main tributary, the Paraguay River, as well as the Uruguay River), Rosendo Mendoza tower 2) the region close to the Atlantic Ocean, Jose Ignacio and 3) the more continental region of the country at least 300 km from the Río de la Plata and the Atlantic Ocean Colonia Rubio. New technological applications of wind power, have provided data at heights previously little studied in the atmospheric boundary layer from 40 to 100 m. Furthermore, new wind energy projects need wind velocity measurements at the height of the axis of a wind turbine [1]. UTE has installed a wind-resource measurement network comprising anemometers and wind vanes, pyranometers and thermometers distributed throughout the country. Wind measurements are made with cup anemometers (model NRG 40) and wind vanes (model NRG 200P). The amplitude of the horizontal wind velocity, sampled at a rate of once every 2 seconds, commercial a data logger installed in tower registered the mean maximum, and standard deviation every 10 minutes. For this work is computed and used in the analysis a hourly data average for the mean, standard deviation. The towers of the measurement network are usually equipped with anemometers with an orthogonal azimuth at various heights so that the effect of tower wake can be determined and removed. The towers selected as representative of these regions are Rosendo Mendoza (RM), Jose Ignacio (JI), Colonia Rubio (CRU) and McMeekan (MC) (Table 1) Figure 1 shows the location of the towers and wind farm analyzed in this work, plotted on the topography of Uruguay.

The land surface is similar at all measurement towers, being open flat grassland with few isolated obstacles. The spatial-temporal behavior of wind speed has been analyzed by [2]. Three towers were selected in the present study by taking into account the regions identified in the cited work. Another criterion for the selection of the three towers was the number of heights at which temperature measurements were made, with a view to investigating stability according to the gradient of temperature. Wind energy is harvested in the region of the planetary boundary layer where diurnal changes associated with heating and cooling are strong. Additionally, depending on the local topography and distance to the sea, different mesoscale processes are observed. According to [3], the convective layer of the atmosphere grows in height throughout the morning,reaching a height of 1--2 km by mid-afternoon. With the approach of sunset, the capping inversion weakens and becomes patchy as one or more shallow inversion layers form below. At this time, there is a rapid collapse of turbulent motion in the boundary layer as the

buoyant plumes that maintain the motion lose their energy source near the surface since the ground cools quickly from radiative heat loss to space.In the present work, the observational data are measurements of the wind velocity and temperature sampled at a frequency of 0.5 Hz and registered by a data logger every 10 minutes. The diurnal cycle of solar radiation thus determines the condition of stability [4]. There are periodical changes in the vertical structure of the region of the atmosphere analyzed in this work over the course of a day. There is a transition between a stable condition and unstable condition during sunrise and sunset. The present work describes the diurnal variations in the gradient of temperature, the gradient of the horizontal velocity, and the intensity of turbulence. To analyze the variations in different seasons of the year in terms of the diurnal cycle, the 10-minute data were processed to obtain the mean and maximum value of each variable in each hour in each season. The analysis is presented by season of 2012 year ---winter, autumn, spring,and summer---because there are significant changes in solar radiation during the year at latitudes of 30 S and 35 S, this will have a explicit presentation in 2.1 . This work presents data analysis for the three observation towers. Further analysis plots the hourly mean value and 16th and 84th percentiles of the different variables computed from the observational data. The impact of intensity of turbulence in power production will be shown qualitative in terms of the diurnal cycle of generation for Kentilux for 2014, this wind farm is one that have a long term historical power production registered.

	Code	Lat South	Long West	Wind velocity measurement height (m)	Temperature Measurement (m)	Radiation measurement	Power Capacity installed (MW)
Kentilux (Wind Farm)	KENT	34,74	56,57	----	----	----	17,2
Colonia Rubio	CRU	31,238	57,465	101-80-60	99-3	yes	----
Jose Ignacio	JI	34,85	54,735	98-40-12	98-4	yes	----
McMeekan	MC	34,643	56,695	101-81-63,5	100-4	yes	----
Rosendo Mendoza	RM	34,275	57,553	101-81-63,5	100-2	----	----

Table 1. Tower and wind farm, locations measurement heights.

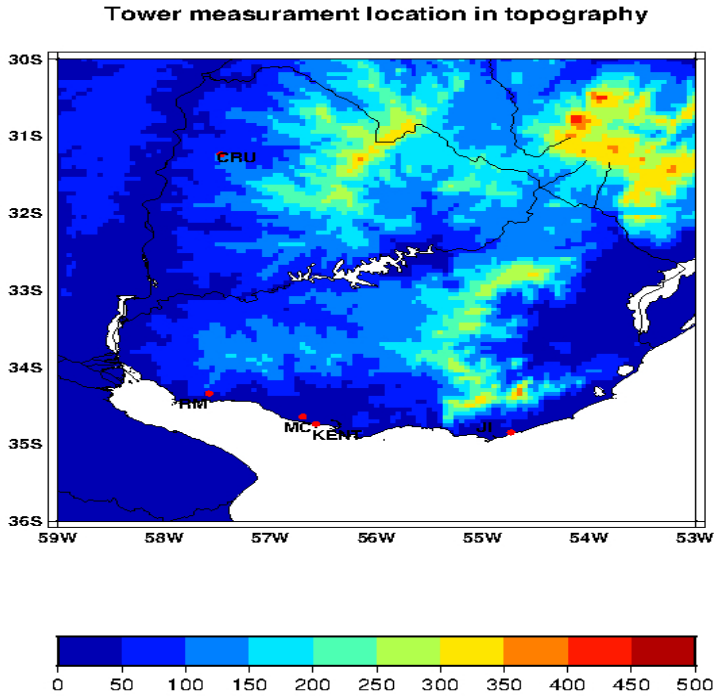

Figure 1 - Locations of six towers considered in this work, and the topography of Uruguay (scale in meters).

2 DIURNAL CYCLE ANALYSES

2.1 Description of solar irradiance variation during different season.

Solar Irradiance measurements are made with Li-Cor LI-200SZ Pyranometer model NRG sampled at a rate of once every 2 seconds, commercial a data logger installed in tower registered the mean maximum, and standard deviation every 10 minutes. For this work is computed and used in the analysis an hourly data average for the mean, standard deviation, and maximum values for each hour. Figure 2, 3 and 4, show the diurnal cycle of solar irradiance (W/m^2) discriminated by season (summer, autumn, winter and spring) at McMeekan, Colonia Rubio and Jose Ignacio towers respectively, hourly mean value and 16th and 84th percentiles.

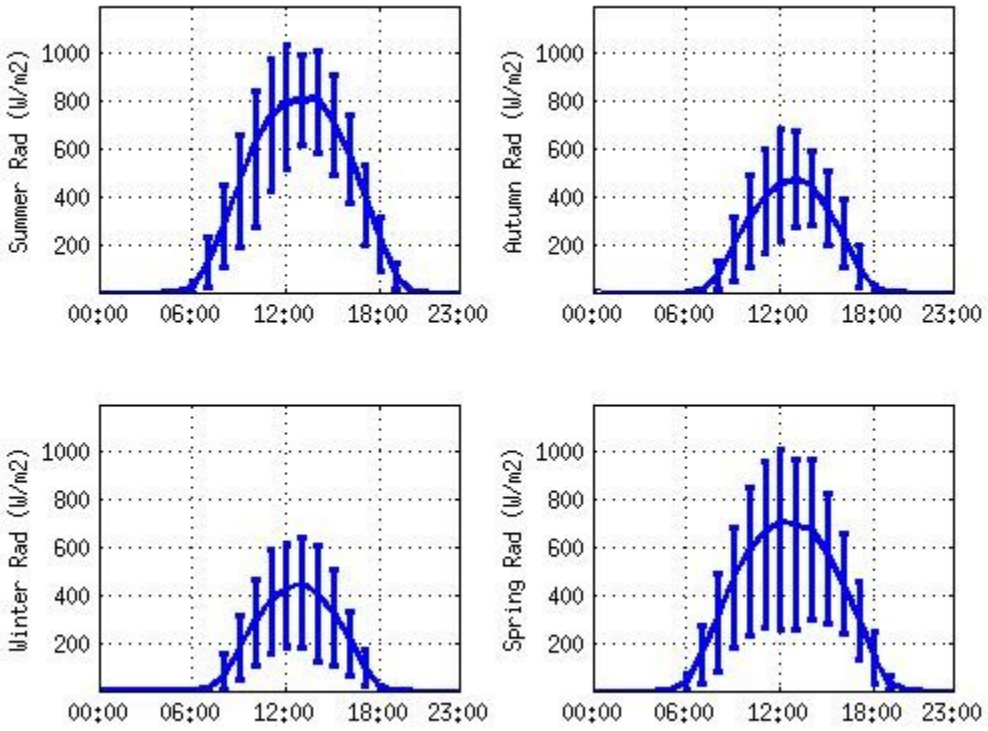

Figure 2 Diurnal variation in the irradiance at the MC tower, in W/m^2. The vertical bars show the mean and 16th and 84th percentiles.

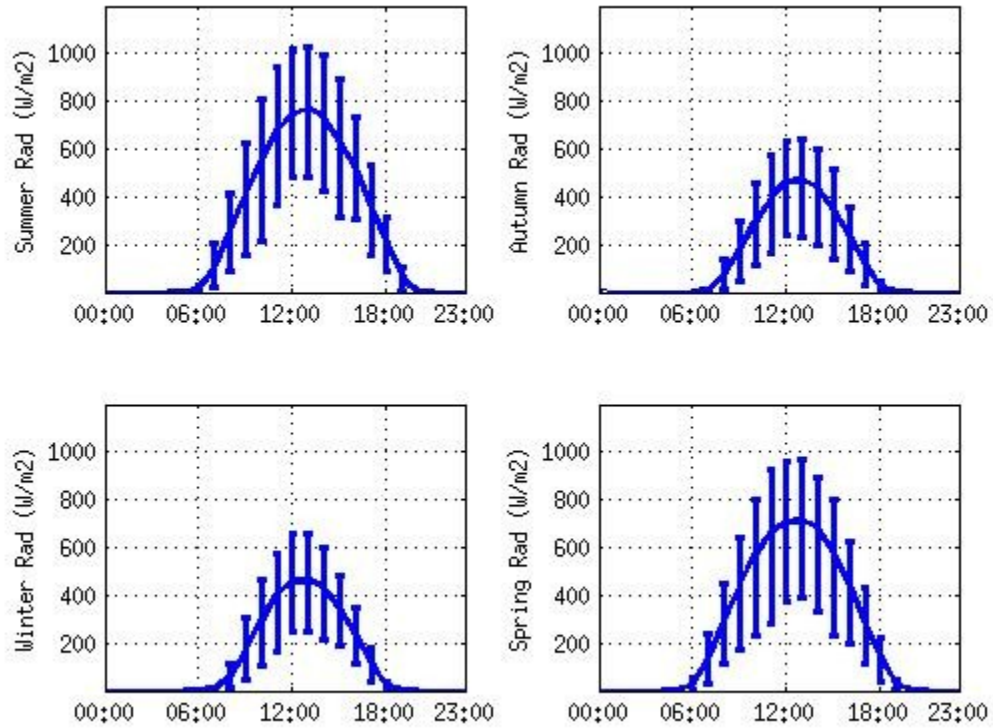

Figure 3 Diurnal variation in the irradiance at the CR tower, in W/m^2. The vertical bars show the mean and 16th and 84th percentiles.

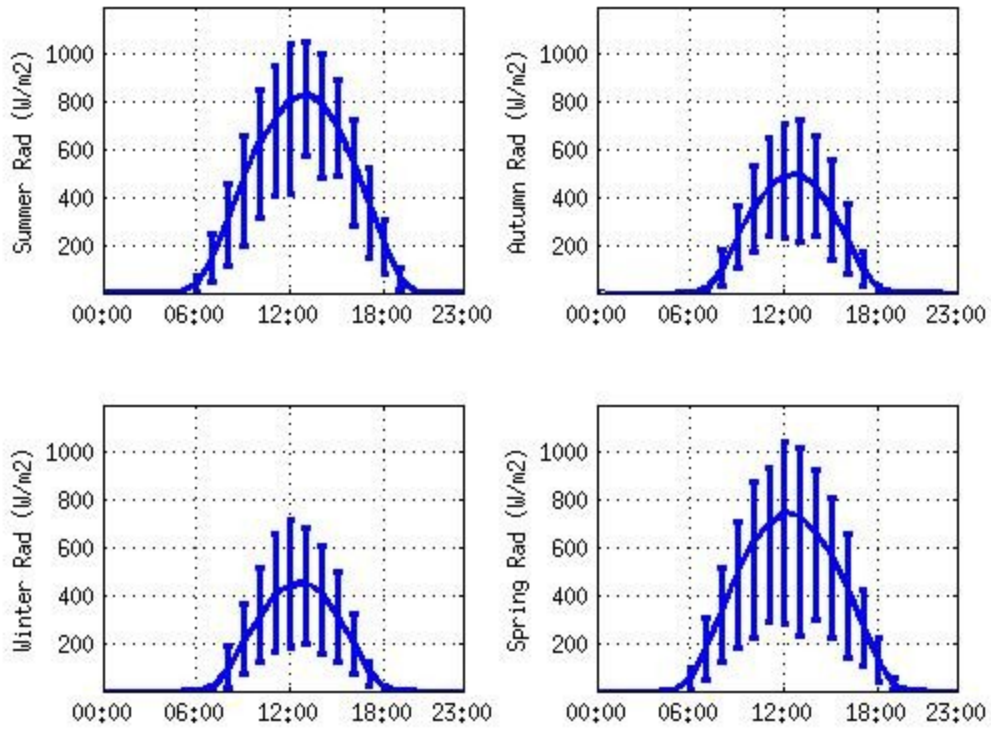

Figure 4 Diurnal variation in the irradiance at the JI tower, in W/m^2. The vertical bars show the mean and 16th and 84th percentiles.

The analysis show there are significant changes in solar radiation during the year at latitudes of 30 S and 35 S---winter, autumn, spring,and summer---.

2.2 Discrimination of the stability regime.

The gradient of temperature is an indicator of atmospheric stability [5]. No measurements of humidity are considered here. The temperature gradient presented in this work covers heights from 2--12 m to 98--101 m above the ground depending on the tower location. The temperature gradient is hardly affected by sensible heat exchange. According to [6], negative heat transfer refers to heat transfer from the atmosphere to the ground (stable regime). The heat transfer is positive when the ground is warmer than the atmosphere (unstable regime). Latent heat is not measured in this work, and only the temperature gradient is used in the discrimination of cases. Plots show clearly different patterns for different meso scale regimes. The adiabatic temperature lapse rate (Γ=-0.0098 °K/m), if the temperature gradient is used as an indicator of stability, a higher positive value indicates a strongly stable regime. A superadiabatic temperature gradient indicates a strongly unstable regime. In the 100 m nearest the ground surface, there is no significant change in the hydrostatic pressure with height, an assumption that the potential temperature is similar to the temperature can be adopted. Figure 5, 6 and 7, show the diurnal cycle of the temperature gradient discriminated by season (summer, autumn, winter and spring) at Rosendo Mendoza, Colonia Rubio and Jose Ignacio towers. Following sunrise, regimes with a superadiabatic temperature gradient are frequently observed.

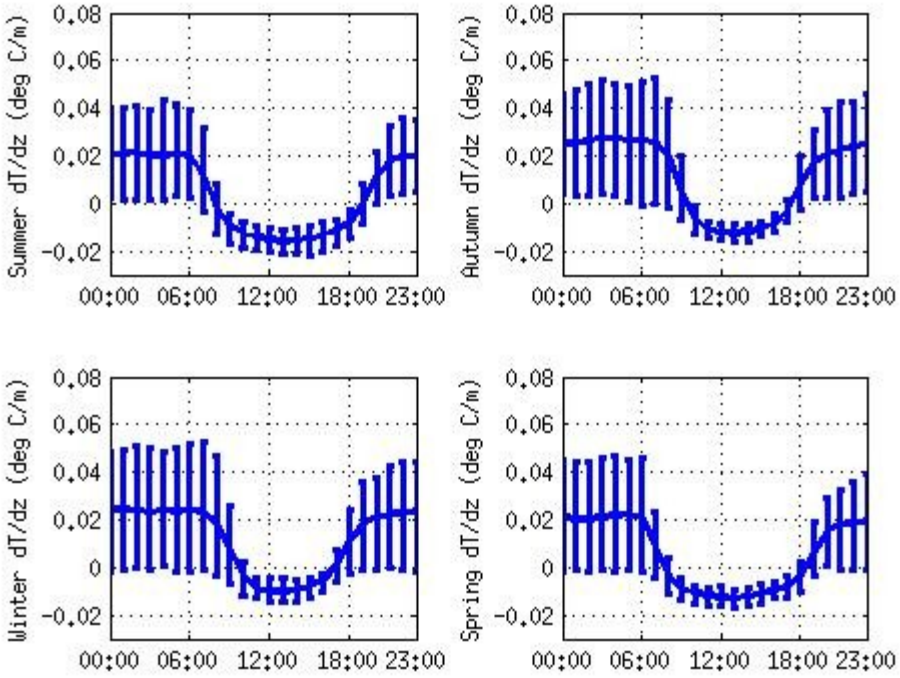

Figure 5 Diurnal variation in the gradient of temperature at the RM tower, at heights between 2 and 100 m, in degrees Celsius per meter. The vertical bars show the mean and 16th and 84th percentiles.

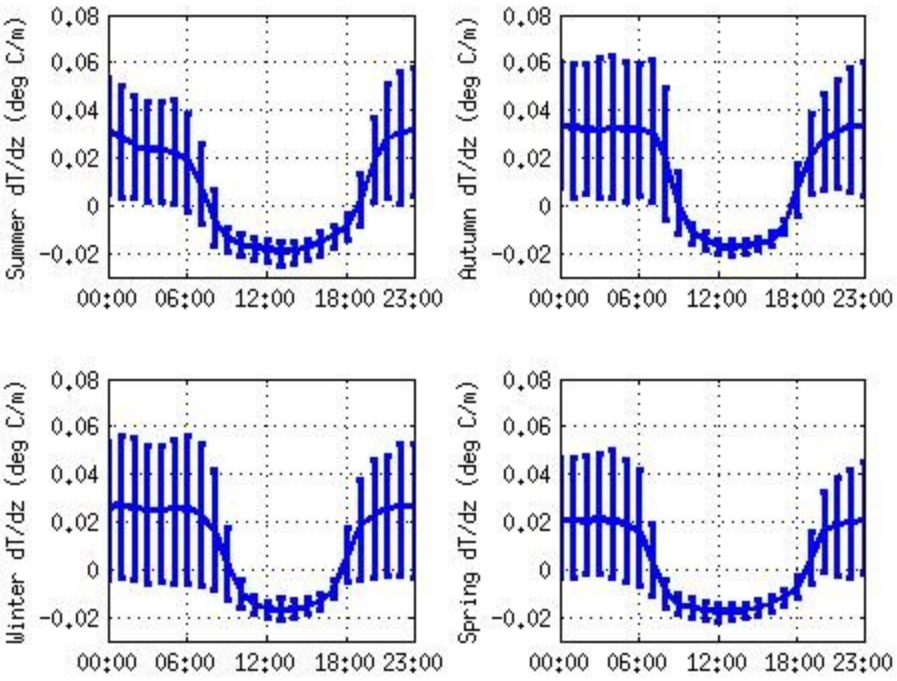

Figure 6Diurnal variation in the gradient of temperature at the CR tower, at heights between 3 and 99 m, in degrees Celsius per meter. The vertical bars show the mean and 16th and 84th percentiles.

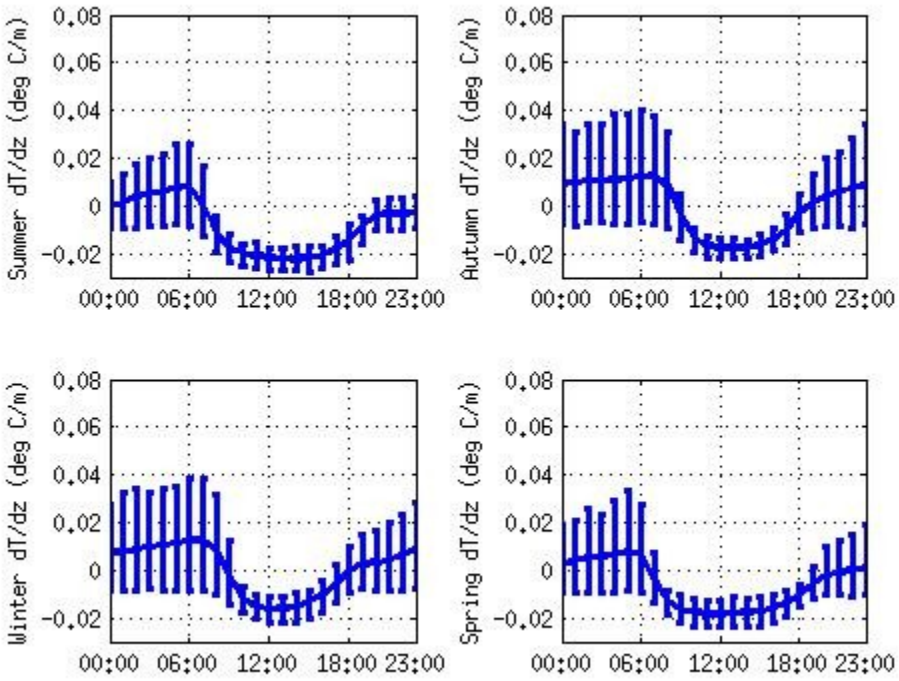

Figure 7 Diurnal variation in the gradient of temperature at the JI tower, at heights between 12 and 98 m, in degrees Celsius per meter. The vertical bars show the mean and 16th and 84th percentiles.

Strong stability is observed at tower locations far from the ocean coast at night. The sea breeze mixes the air at different levels. Mean values of solar radiation for the analyzed region [7] show that the east coast closer to the ocean receives less radiation during the day, which is related to the higher probability of cloud cover. If the same relation holds at night, the cloud cover implies less stability in Jose Ignacio than on Colonia Rubio or Rosendo Mendoza.

2.3 Vertical gradient of horizontal wind

This work compares the wind velocity gradients $\frac{\delta V}{\delta z}$ (1/s) at different locations for similar measurement heights of a cup anemometer.

As described previously, the temperature gradient strongly correlates with the diurnal cycle of solar radiation, and there are thus buoyancy forces that affect the wind profile. The gradient of horizontal velocity calculated from the measurements made by cup anemometers at different heights shows the variation in the wind profile during the diurnal cycle Figure 8, 9 and 10 show the diurnal cycle of the velocity gradient at different levels discriminated by season (summer, autumn, winter and spring) at Rosendo Mendoza, Colonia Rubio and Jose Ignacio towers.

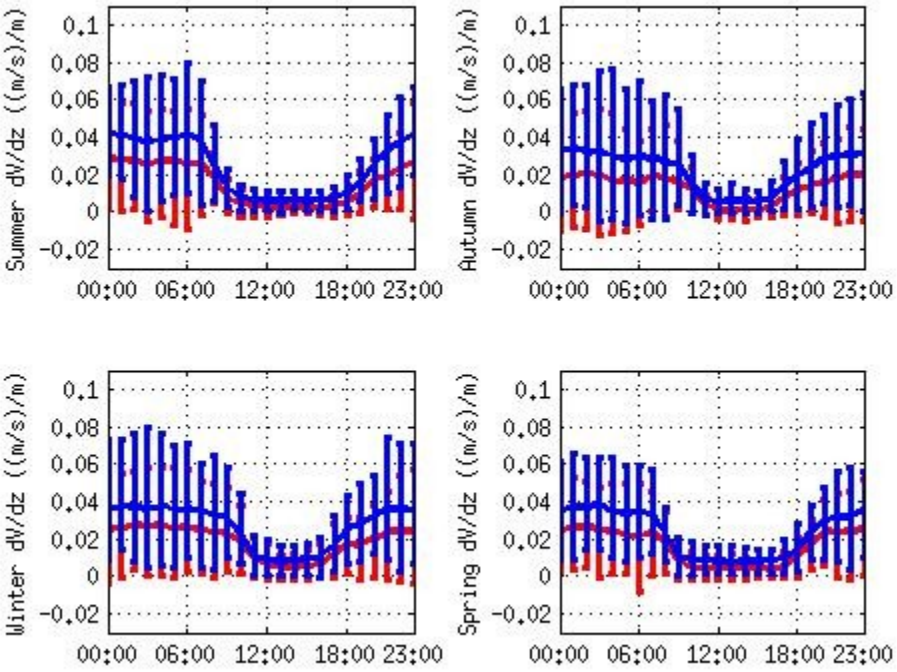

Figure 8. Diurnal variation in the gradient of velocity discriminated by season (summer, autumn, winter and spring) at Rosendo Mendoza tower, between 63,5 and 81 m (blue) and between 81 and 101 m (red). The vertical bars show the mean and 16th and 84th percentiles.

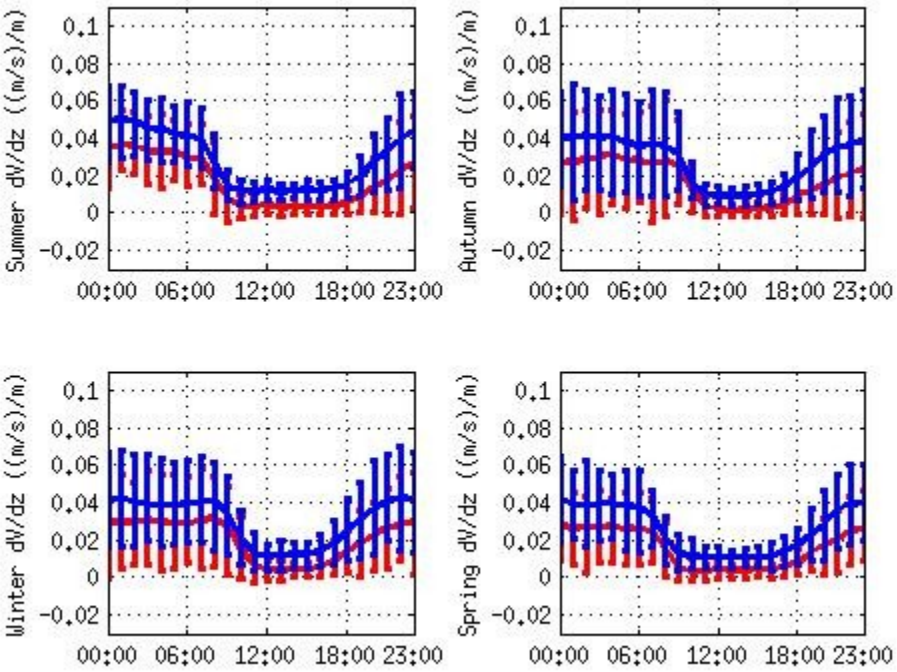

Figure 9. .Diurnal variation in the gradient of velocity discriminated by season (summer, autumn, winter and spring) at Colonia Rubio tower, between 60 and 80 m (blue) and between 80 and 101 m (red) in units of (1/s). The vertical bars show the mean and 16th and 84th percentiles.

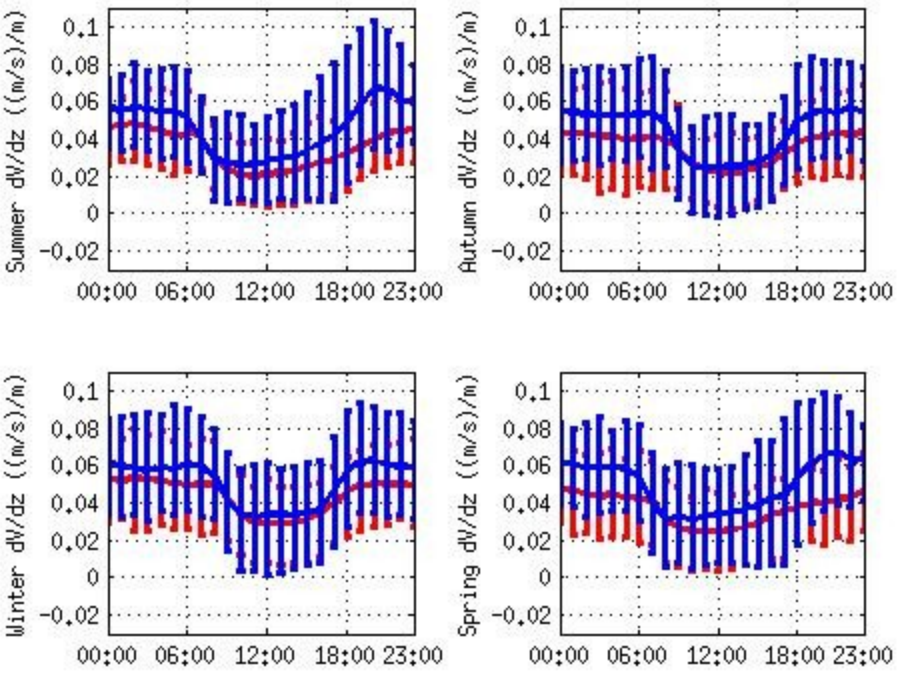

Figure 10. Diurnal variation in the gradient of velocity discriminated by season (summer, autumn, winter and spring) at at Jose Ignacio tower, between 12 and 40 m (blue) and between 40 and 98 m (red). The vertical bars show the mean and 16th and 84th percentiles.

During the night and at heights between 60 and 100 m, the velocity gradient ranges $0<\frac{\delta V}{\delta z}<0{,}08$ (1/s) between the 16th and 84th percentiles. The range and values of the velocity gradient are greater than those of the velocity gradient after sunrise, $0<\frac{\delta V}{\delta z}<0{,}02$ (1/s)

Closer to the ground, the velocity gradient on the oceanic coast has a larger spread and higher values, and there is less contrast between night and day in the diurnal cycle, thus can be related with sea breeze related with water ocean mass.

2.4 Mean velocity.

As was shown in the analysis presented in 2.3 the vertical gradient of horizontal wind shows that during unstable condition there is tendency of have a uniformity velocity in *swept area* of *wind* turbines blades heights. Figures 11, 12 and 13 shows diurnal variation of mean velocity for the top and bottom height measured, discriminated by season (summer, autumn, winter and spring) at Rosendo Mendoza, Colonia Rubio and Jose Ignacio towers.

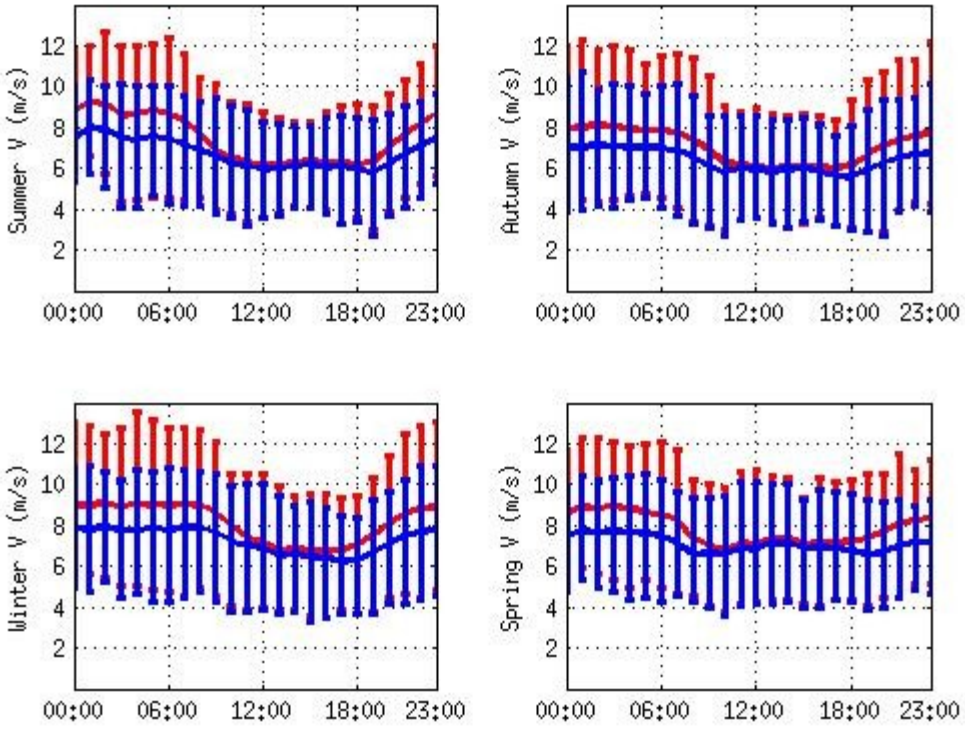

Figure 11. Diurnal variation of mean velocity discriminated by season (summer, autumn, winter and spring) at Rosendo Mendoza tower, between 63,5 m (blue) and 101 m (red) in units of (m/s). The vertical bars show the mean and 16th and 84th percentiles.

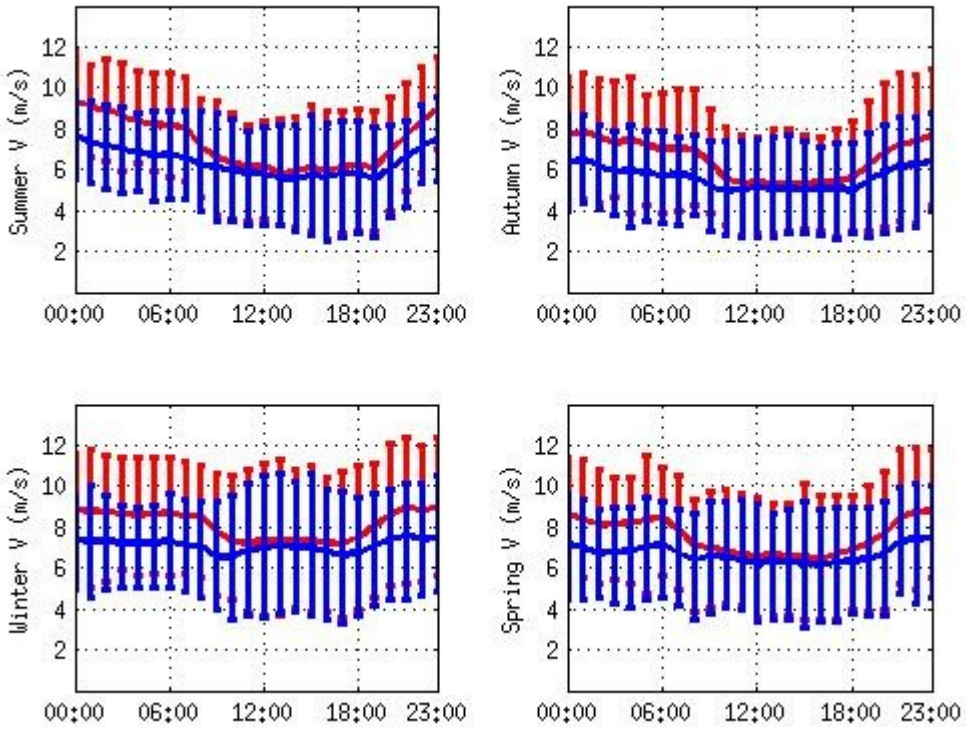

Figure 12. The vertical bars show the mean and 16th and 84th percentiles.Diurnal variation in velocity discriminated by season (summer, autumn, winter and spring) at Colonia Rubio tower, between 60 m (blue) and 101 m (red) in units of (m/s). The vertical bars show the mean and 16th and 84th percentiles.

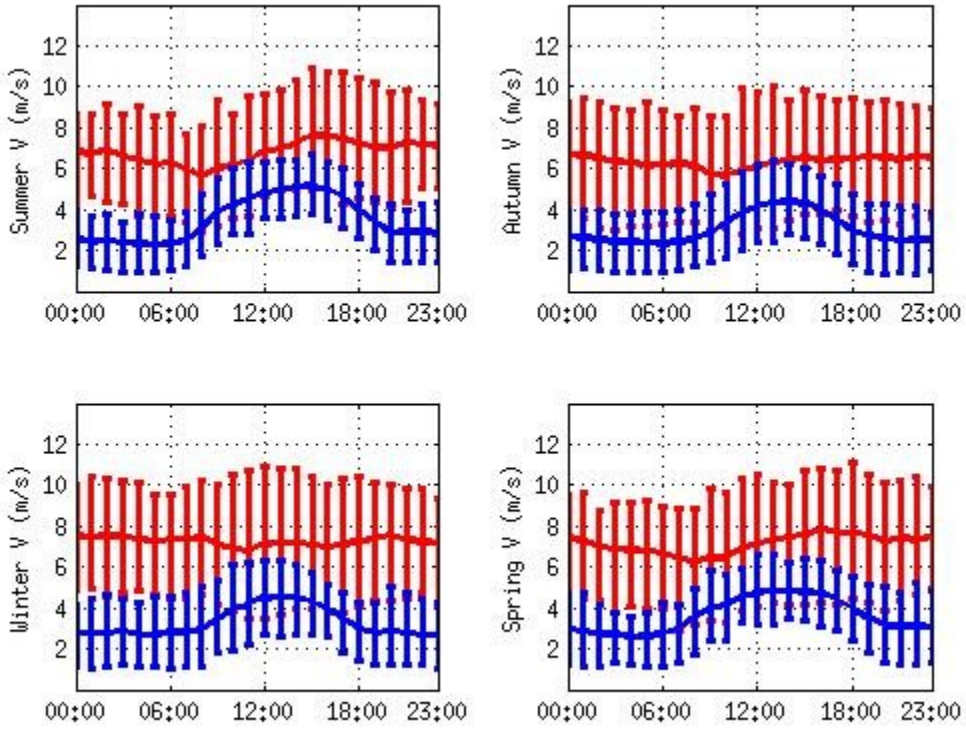

Figure 13. Diurnal variation of velocity discriminated by season (summer, autumn, winter and spring) at at Jose Ignacio tower, between 12 m (blue) and 98 m (red) in units of (m/s).

Top level measured have minimum values during unstable regimes, the thermal vortex produce strong mixing then lowest level increase the mean velocity and highest level decrease, then during stable regimes night time, as was seen in vertical gradient of velocity the difference in velocity between higher an lowest levels have a significant increase.

2.5 Intensity of turbulence.

The turbulence intensity *IT* (1) is defined as the standard deviation divided by the mean velocity. *IT* is a factor relevant for the description of the wind load, and wind turbines classes selection in reference to this parameter that describes the nature of the wind energy resource in analyzed places. Also can be a parameter for wind energy production that can describe the regime that is present in the conversion of the kinetic energy by wind turbine, then power curve can be parametrized with a long term data historical production of power, mean velocity and intensity of turbulence. *IT* in gust analysis is a measure of the weight of turbulence in a gust. *IT* describe the mean fluctuation of the mean velocity measured in tower, is a measure of turbulence in a "bulk" statistical description, more related with large scales of turbulence.

$$IT = \frac{\sigma}{\bar{V}} \quad (1)$$

Figure 14, 15 and 16 shows diurnal variation discriminated by season (summer, autumn, winter and spring) of *IT* at, Rosendo Mendoza Colonia Rubio and Jose Ignacio towers. The peak of intensity of turbulence is related with unstable state associated with thermal production of turbulence produced by buoyancy. The plots shows IT variation for the top height measured in each tower analized to have results that can be assimilated with the same physical process related with change in stability regime in *swept area* of *wind* turbines blades heights.

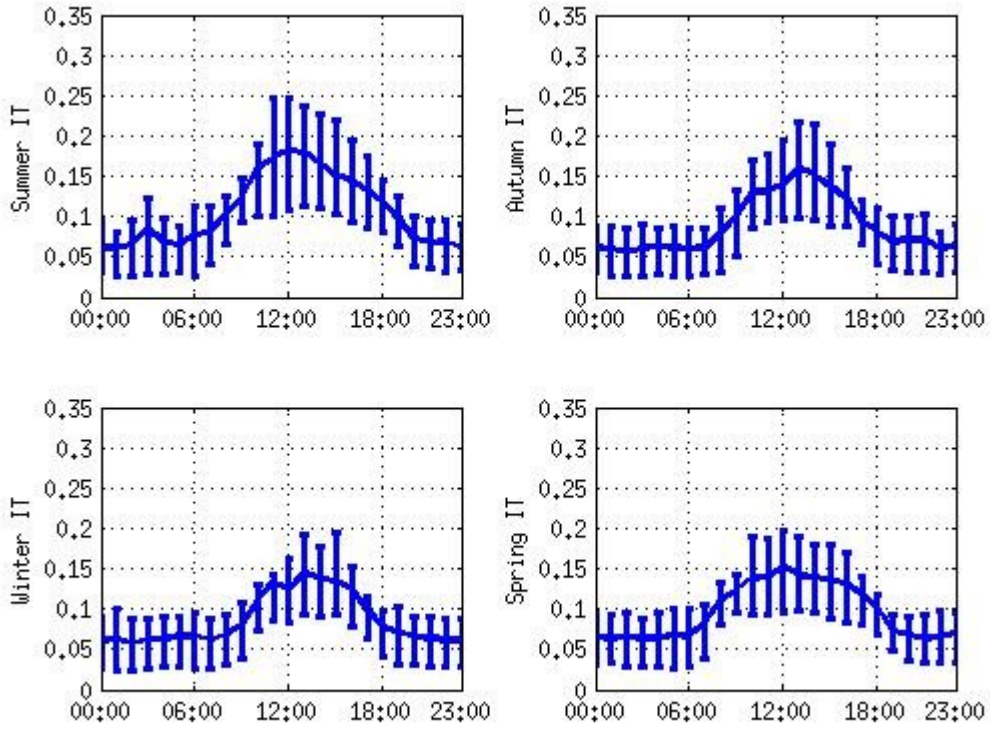

Figure 14. Diurnal variation discriminated by season (summer, autumn, winter and spring) of IT at Rosendo Mendoza tower, at a height of 101 m. The vertical bars show the mean and 16th and 84th percentiles.

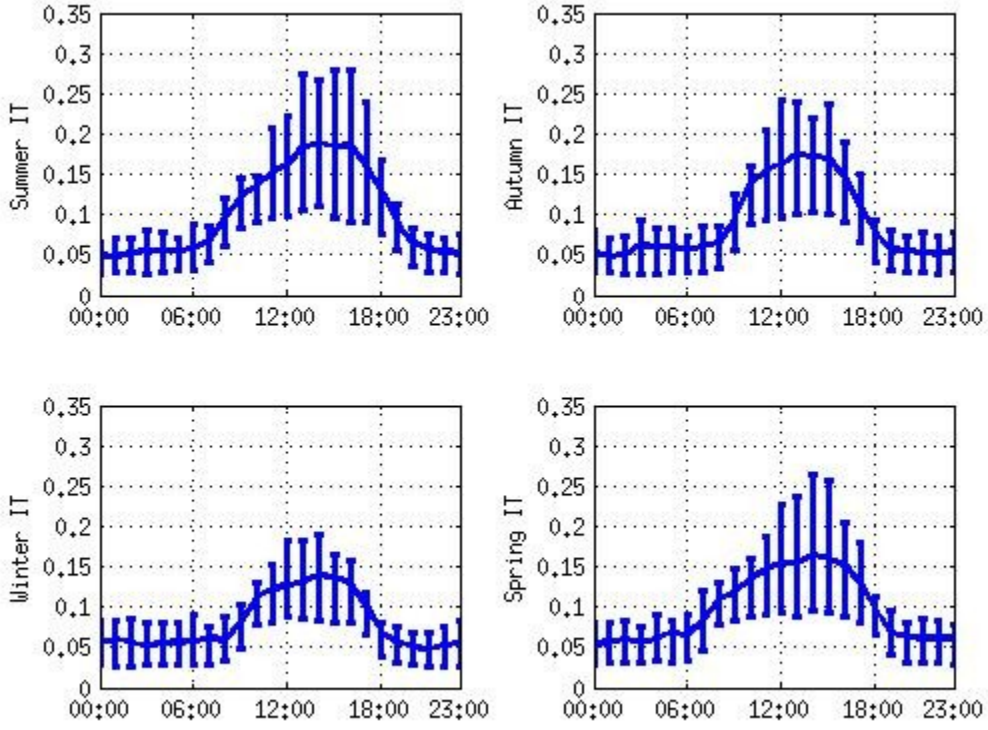

Figure 15. Diurnal variation discriminated by season (summer, autumn, winter and spring) of IT Colonia Rubio tower, at a height of 101 m. The vertical bars show the mean and 16th and 84th percentiles.

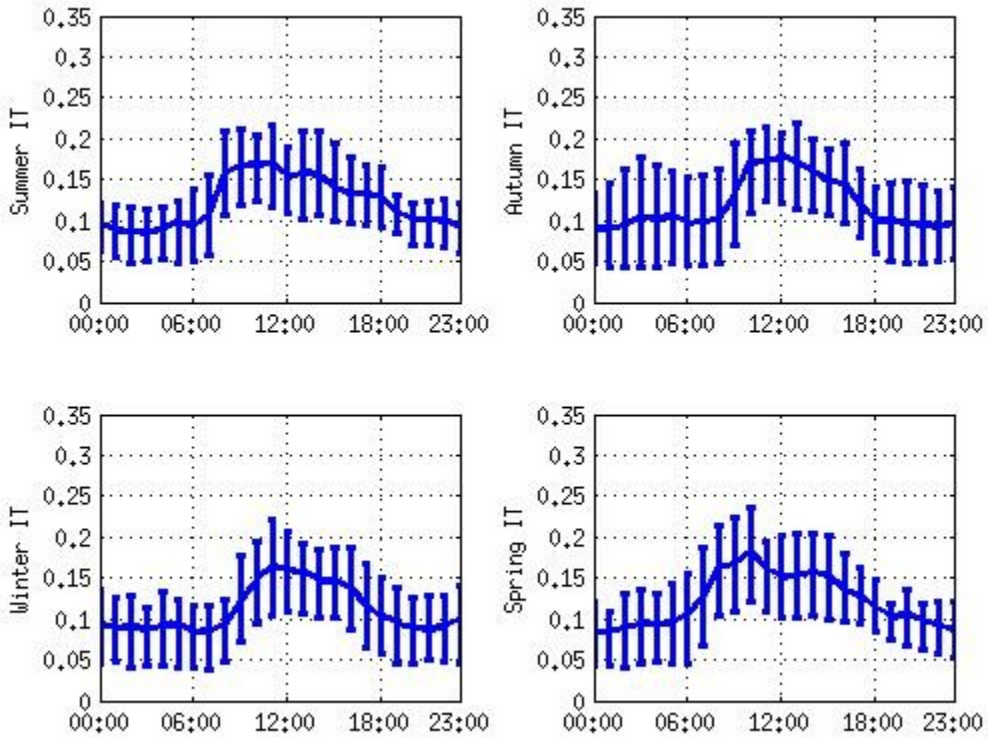

Figure 16. Diurnal variation discriminated by season (summer, autumn, winter and spring) of IT Jose Ignacio tower, at a height of 98. The vertical bars show the mean and 16th and 84th percentiles.

The local vertical stability at each tower is both directly assessed from differential temperature measurements (using thermometers mounted near tower top and bottom). Four stability classes are defined empirically as:

1. Unstable when $\frac{\delta T}{\delta z}$ < -0.01 °C/m, red in plots.
2. Slightly unstable when 0 °C/m > $\frac{\delta T}{\delta z}$ > -0.01 °C/m, magenta in plots.
3. Slightly stable when 0.01 K/m > $\frac{\delta T}{\delta z}$ > 0 °C/m, blue in plots.
4. Stable when $\frac{\delta T}{\delta z}$ > 0.01 °C/m, green in plots.

Figure 17 shows a scatter plot of turbulence intensity versus mean velocity discriminated by at Rosendo Mendoza, Colonia Rubio and Jose Ignacio towers, for top and bottom velocity height measured in each tower.

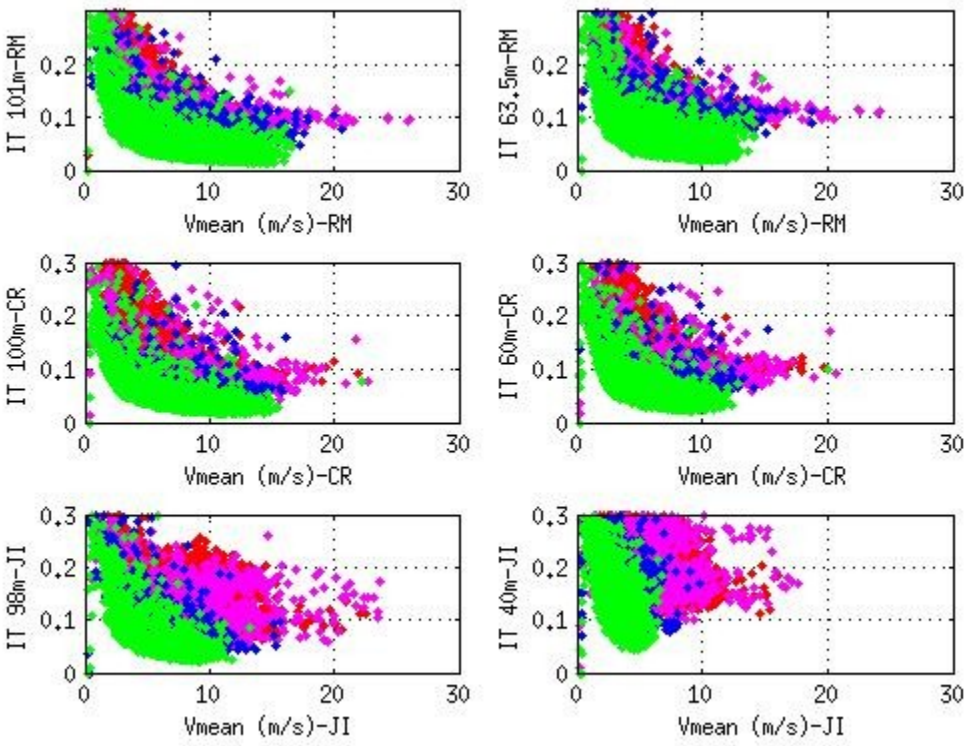

Figure 17. scatter plot of turbulence intensity versus mean velocity discriminated by at Rosendo Mendoza, Colonia Rubio, and Jose Ignacio towers, data are color-coded by vertical stability measured at the towers.

The *IT* have a more significance dispersion in ocean coast tower for the gusty cases with higher mean wind velocity, when mean velocity is extreme the stability condition is slightly unstable,and the *IT* tend to reach a clear asymptotic value of *IT*=0,1 for Rosendo Mendoza and Colonia Rubio. Strong wind condition are associated with unstable regime conditions.

2.6 Power production of Kentilux wind farm.

There are currently only two wind farms with new technology and long-term power generation in Uruguay, Emanuelle Cambilargiu and Kentilux.

Kentilux is on relatively flat terrain, whereas Emanuelle Cambilargiu is atop a ridge with relatively steep slopes. Electrical energy produced and input to the electrical grid is from the transformation of available kinetic energy in the atmospheric boundary layer from airflow. Thus, it is of interest to conduct numerical simulation of the near-surface atmosphere. All the results presented associated with wind measurement described flat plate terrain diurnal cycle so, Kentilux wind farm was selected for the present analysis. The Kentilux wind farm is on the Río de la Plata coastline San Jose, Uruguay. This farm is currently composed of five wind turbines of model Vestas V90-2 MW and four Vestas V100-1.8 MW, with total installed power of 17.2 MW.

The factor of capacity of a wind farm (2) is defined as the ratio of the mean wind power generation in an hour $\bar{P}$ and the total nominal power installed $P_{installed}$.

$$FC = \frac{\bar{P}}{P_{installed}} \quad (2)$$

Figure 18 shows the factor of capacity for Kentilux wind farm for the total year 2014, the data used come form SCADA automatic acquisition system of UTE, there is no information available by the author in the time was written this work of *availability* of wind turbine, so the plot show the raw data of production of wind farm analyzed.

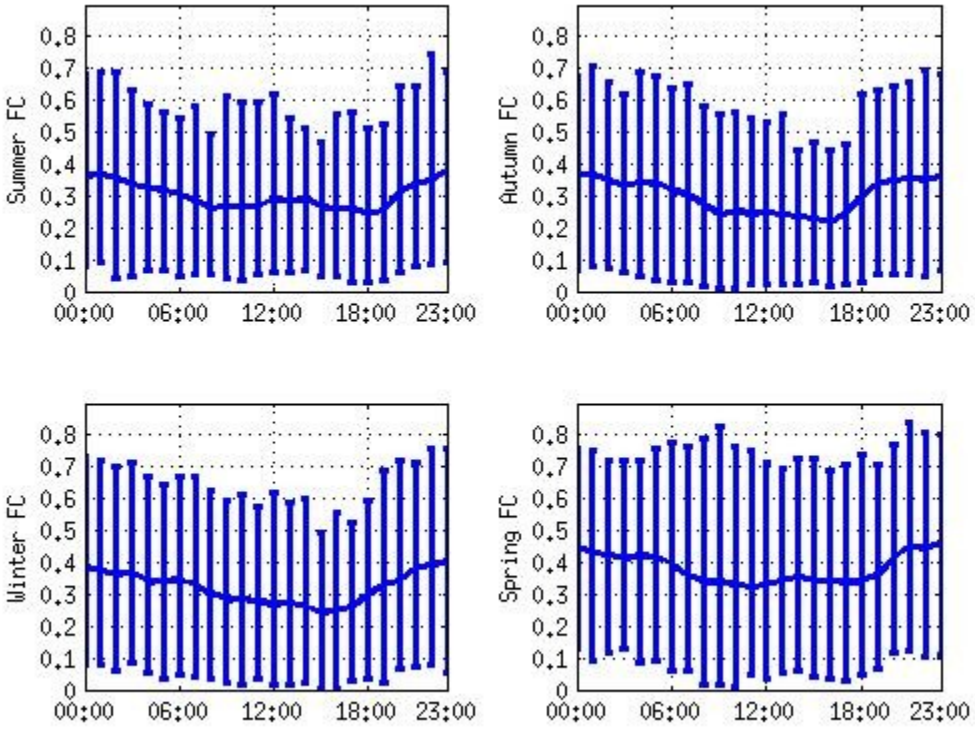

Figure 18. Kentilux wind farm mean factor of capacity, for 2014 year. The vertical bars show the mean and 16th and 84th percentiles.

[8] present the incidence of intensity of turbulence in wind power production, the authors based in 3 months measurement period, results show behavior of the power curve related to both turbulence intensity and wind shear. The cases piloted in this work show that high *IT* tends to have associated less wind power production.

During day time and night time 2.3, 2.4 and 2.5 show a clear different wind profile and stability regime and intencity of turbulence diurnal cycle. The present results fig 18, show that the mean factor of capacity have a the minimum values during unstable regimes, thus represent a diminish in power production at day time, that can be related both in diminish of mean velocity at *swept area* of *wind* turbines blades heights, and the increase of intensity of turbulence. Further analysis need to be done with long term wind power production, for a more clear understanding of the mechanical exchange of energy at *swept area of wind turbines.* Model output statistic with goal in wind energy forecast, can use IT and mean velocity as parameter for calibration, in next chapter is presented a WRF simulation with the goal of forecast IT.

3 NUMERICAL SIMULATION OF INTENSITY OF TURBULENCE

[9] uses large-eddy simulation (LES) to explore properties of the stable boundary layer (SBL) using an explicit filtering and reconstruction turbulence modeling approach, this work focus in a full scale description of turbulence for wind energy propose. The present work uses a conceptual different approach working with WRF simulation, the simulation focus in large scale of turbulence description associated with mean fluctuation of mean velocity, that can be described with *IT.*

3.1 WRF simulations.

Nested simulations are targeted to each of the three towers separatel three domain each 30 km-10km-3,3km. In each model run, the nesting is two-way and the 30-km domain covers a significant portion of South America (not shown), centered on the Rio de la Plata, with the finer domains centered on the tower locations. Separate model runs employing one, two, three and all four domains were made. All simulations utilize 53 vertical layers with the model top at 100 hPa. The lowest model sigma levels are at 1, 0.9987, 0.9974, 0.9948, 0.9922, 0.9896, 0.98693, 0.9843 and 0.9777. Physical parameterizations selected for these runs include the National Center for Atmospheric Research (NCAR) Community Atmospheric Model (CAM) radiation scheme [10], Purdue-Lin microphysics [11], and the Noah land surface model [12]. The Kain-Fritsch [13] cumulus parameterization is employed in the 30- and 10-km domains. The National Centers for Environmental Prediction (NCEP) Global Forecast System (GFS) operational global analyses are used for the initial and boundary conditions. Sensitivity to the number of domains used and the planetary boundary layer scheme (PBL) was assessed, with the Mellor-Yamada-Janjic (MYJ) scheme [14] representing the control configuration examined herein.

3.2 Proposed IT model based in WRF

In this work it is proposed the relation (3), for modeling *IT* based in WRF, where *ust* is computed friction velocity by WRF and $\bar{V}$ is computed mean velocity by WRF (mean velocity in second level (92m)), k_{IT} is dimensionless coefficient that is computed for each tower.

$$IT = k_{IT} \frac{ust}{\bar{V}} \quad (3)$$

Best fit coefficients k_{IT} (table 2) for simulation of observed IT are presented in plots Figures 19, 20 and 21 (shows measured *IT* (blue) computed *IT* by WRF (red)), discriminated by season (summer, autumn, winter and spring) at Rosendo Mendoza, Colonia Rubio and Jose Ignacio towers, 2012 year.

Tower	k_{IT}
Rosendo Mendoza	1,65
Colonia Rubio	1,55
Jose Ignacio	2,05

Table 2. k_{IT} is dimensionless coefficient that is computed for WRF simulation in RM, CR and JI.

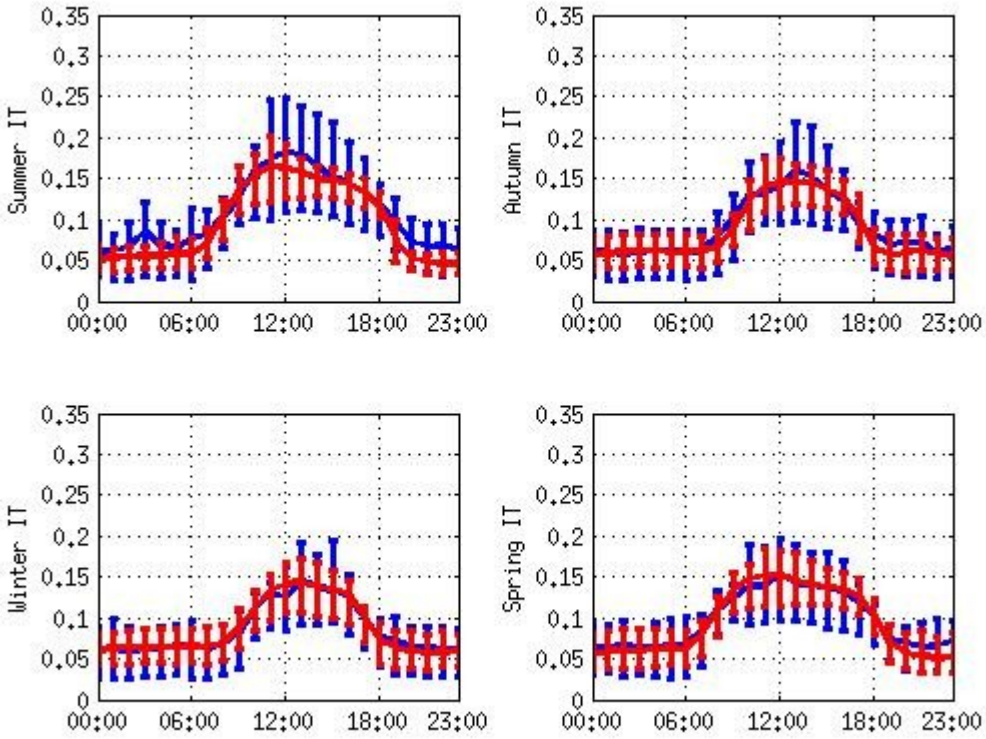

Figure 19. Diurnal variation discriminated by season (summer, autumn, winter and spring) of measured *IT* (blue) computed *IT* by WRF (red) at Rosendo Mendoza tower, at a height of 101 m. The vertical bars show the mean and 16th and 84th percentiles.

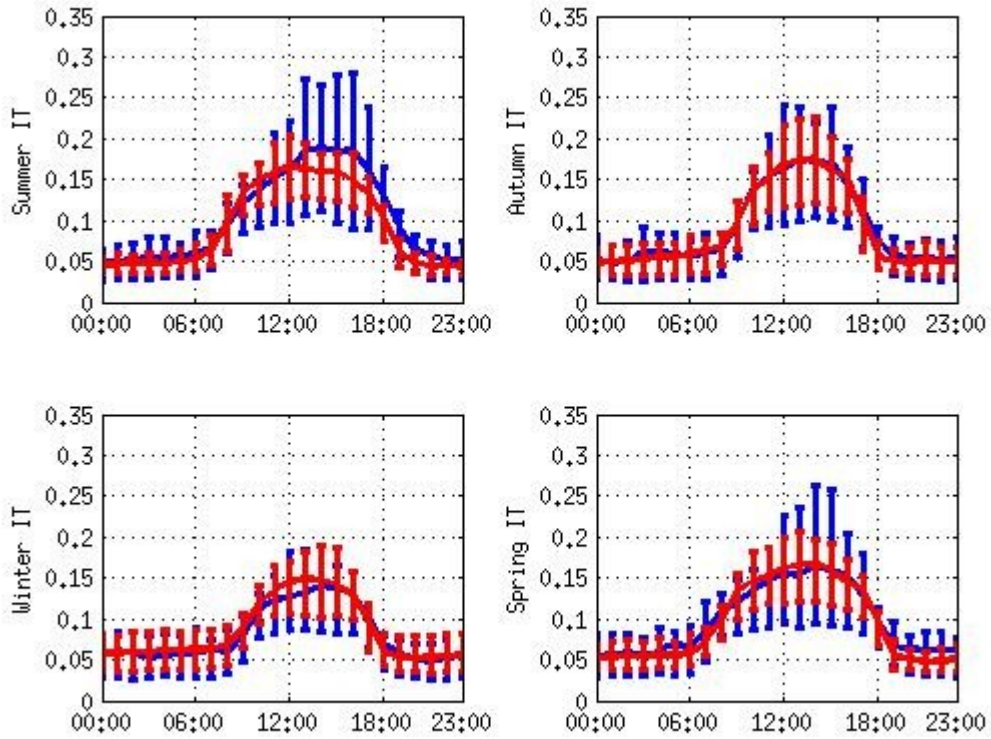

Figure 20. Diurnal variation discriminated by season (summer, autumn, winter and spring) of measured *IT* (blue) computed *IT* by WRF (red) at Colonia Rubio tower, at a height of 100 m. The vertical bars show the mean and 16th and 84th percentiles.

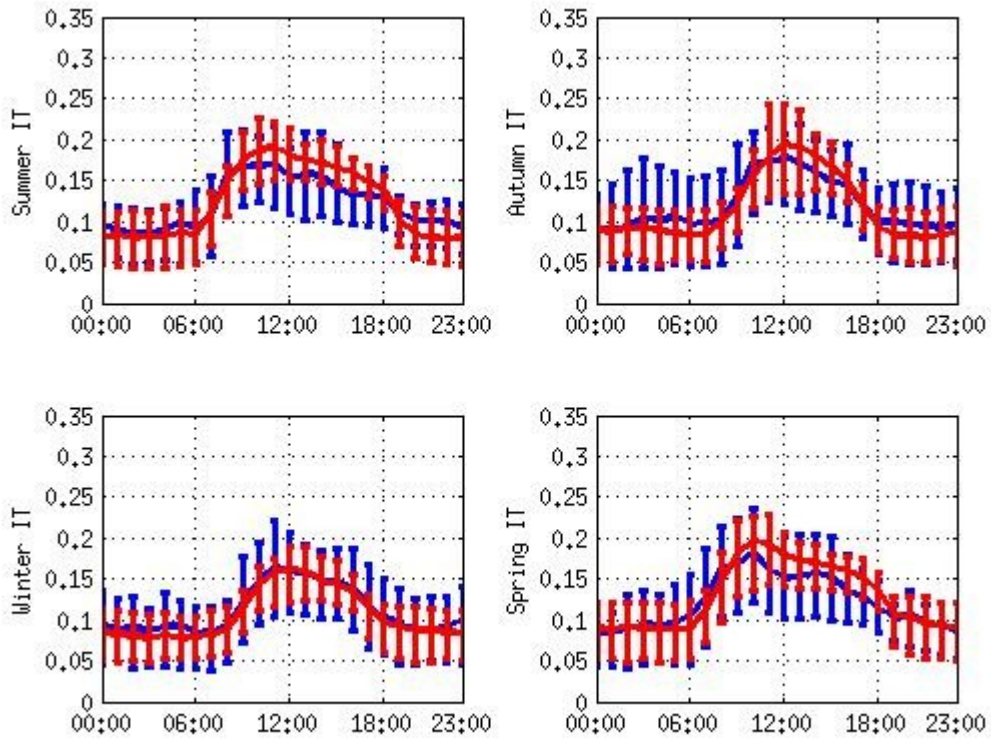

Figure 21. Diurnal variation discriminated by season (summer, autumn, winter and spring) of measured *IT* (blue) computed *IT* by WRF (red) at Jose Ignacio tower, at a height of 98 m. The vertical bars show the mean and 16th and 84th percentiles.

From the simulations, is compute $\frac{\delta T}{\delta z}$ the vertical temperature gradient between the second and first model levels (being roughly 92 and 27 m AGL), noting that these roughly correspond to heights at which the tower thermometers have been mounted (see Table 1). Figure 22 show scatterplots for towers RM, CR, and JI of: a) observed mean velocity vs. observed *IT*; b) WRF simulated mean velocity vs. *IT* computed with (3) .

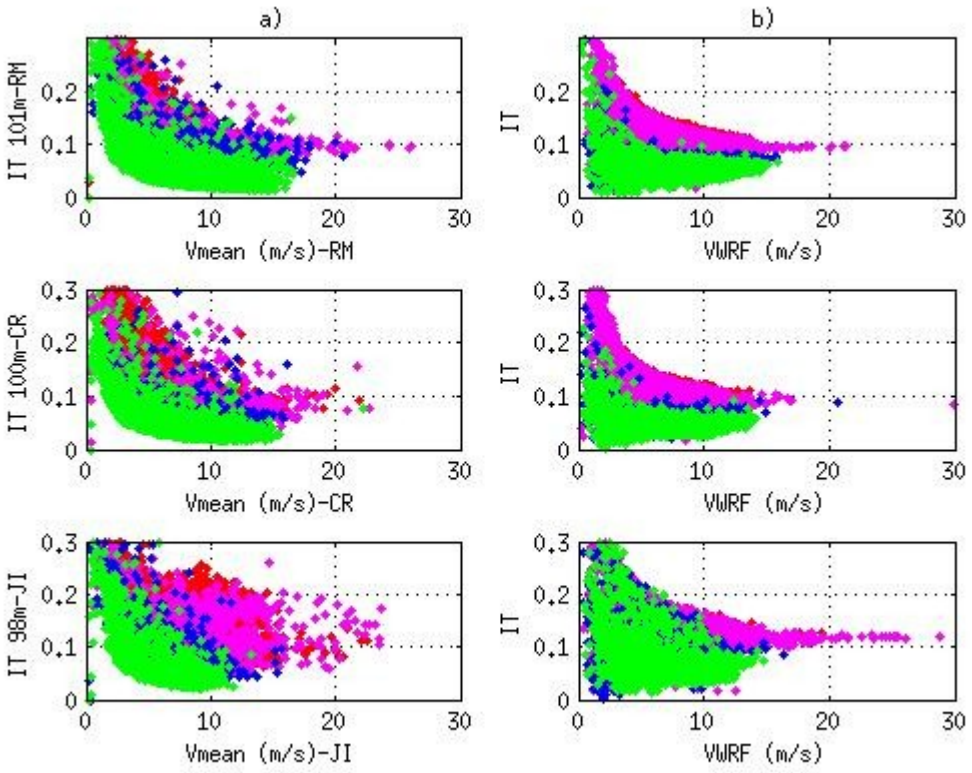

Figure 22. Scatterplots for towers RM, CR, and JI of: a) observed mean velocity vs. observed *IT*; b) WRF simulated mean velocity vs. *IT* computed with (3) In a), data are color-coded by vertical stability measured at the towers; in b), data are color-coded with respect to stability forecasted with WRF..

The propose model show that diurnal cycle of *IT* can be simulated with WRF, also the stability regime can be simulated, the mesoscale regimes related with local condition, can be incorporate in the adjustment of k_{IT} dimensionless coefficient.

CONCLUSION

The present work analyzes wind measurements made for wind energy, the analysis focuses on the mean velocity of at heights between 40 and 100 m, at *swept area* of a *wind* turbines blades . States of stability are discriminated by the vertical gradient of temperature. The diurnal variation of stability is computed and compared among locations with different mesoscale conditions, continental, ocean coast, and estuary coast locations. After sunrise, regimes with a superadiabatic gradient of temperature are observed frequently, with a small spread compared with the gradients of stable regimes at night. Intensity of Turbulence *IT* is described in dependence with stability regimes, for different season. Strong stability is observed at tower locations far from the ocean coast at night. The peak of intensity of turbulence *IT* is related with unstable regimes. *IT* have a more significance dispersion in ocean coast tower, when mean velocity is extreme the stability condition is slightly unstable,and the *IT* tend to reach a clear asymptotic value of 0,1 for two tower analyzed Rosendo Mendoza and Colonia Rubio. Also in this work it is proposed a model for computing *IT* based in numerical simulation, with the ratio between *ust (*friction velocity) and mean velocity $\bar{V}$ computed by WRF,a k_{IT} dimensionless coefficient is defined for better adjust related with local mesoscale regimes. The propose model show that diurnal cycle of *IT* can be simulated with WRF, also the stability regime can be simulated, the mesoscale regimes related with local condition, can be incorporate in the adjustment of k_{IT} is dimensionless coefficient

ACKNOWLEDGMENTS

The present results were from recent advances of an agreement for implementation of a forecast system of wind energy power input to the national grid between the Administración Nacional de Usinas y Trasmisiones Eléctricas (UTE) and IMFIA-FING-UdelaR.

REFERENCES

[1] IEC. 61400-12. First edition. 1998-02. Wind turbine generator systems . Part 12: Wind turbine power performance testing
[2] Cornalino Eliana, Martín Draper. Planning the distribution of wind farms in Uruguay in order to optimize the operability of large amounts of wind power. EWEA 2012 Annual Event Monday 16 - Thursday 19 April 2012 | Bella Center, Copenhagen, Denmark http://www.ewea.org/annual2012/
[3] Kaimal, J. C., J. J. Finnigan, Atmospheric Boundary Layer Flows. Their Structure and Measurement, Oxford University Press 1994.
[4] J.C Kaimal, J. C. Wyngaard, D. A. Haugen, O. R. Coté, Y. Izumi, S. J. Caughey, and C. J. Readings, 1976: Turbulence Structure in the Convective Boundary Layer. *J. Atmos. Sci.*, **33**, 2152–2169.
[5] Arya, S. Pal (1998). Air Pollution Meteorology and Dispersion (1st Edition ed.). Oxford University Press. ISBN 0-19-507398-3.
[6] Monin, A.S. and A.M. Obukhov, 1954: Basic laws of turbulent mixing in the surface layer of the atmosphere. Contrib. Geophys. Inst. Acad. Sci., USSR, (151), 163 187 (in Russian).
[7] Gonzalo Abal, Mauro D' Angelo, José Cataldo, Alejandro Gutiérrez. Mapa Solar del Uruguay Versión 1.0 Memoria Técnica. 2011. ISBN 978-9974-0-0847-2.
[8] A. Honrubia, A. Vigueras-Rodríguez, and E. Gómez-Lázaro The Influence of Turbulence and Vertical Wind Profile in Wind Turbine Power Curve 2012 Progress in Turbulence and Wind Energy IV, 251-254
[9] Bowen Zhou · Fotini Katopodes Chow Turbulence Modeling for the Stable Atmospheric Boundary Layer and Implications for Wind Energy. Flow Turbulence Combust (2012) 88:255–277 DOI 10.1007/s10494-011-9359-7
[10] Collins W.D et al 2004: Description of the NCAR Community Atmosphere Model (CAM 3.0), NCAR Technical Note, NCAR/TN-464+STR, 226pp
[11] Lin, Y.-L., R. D. Farley, and H. D. Orville, 1983: Bulk parameterization of the snow field in a cloud model. J. Climate Appl. Meteor., 22, 1065-1092.
[12] Chen, F., and J. Dudhia, 2001: Coupling an advanced land-surface/ hydrology model with the Penn State/ NCAR MM5 modeling system. Part I: Model description and implementation.Mon. Wea. Rev., 129, 569?585.
[13] Kain, J. S., 2004: The Kain-Fritsch convective parameterization: An update. J. Appl. Meteor., 43, 170?181.
[14] Mellor, G. L., and T. Yamada, 1982: Development of a turbulence closure model for geophysical fluid problems. Rev. Geophys. Space Phys., 20, 851-875.